Emmons, H. W., "The Continuum Properties of Fiber Suspensions," *ibid.*, **48**, 679 (1965).
Fan, L. T., and W. S. Hwang, "Dispersion of Ostwald-de Waele Fluid in Laminar Flow Through a Cylindrical Tube," *Proc. Roy. Soc. (London)*, **A283**, 576 (1965).
Fogelberg, B. C., and M. Johanson, "The Use of Radioactive Tracers in Investigations into Bleaching Process," *Paperi ja Puu*, **40**, 571 (1958).
Forgacs, O. L., A. A. Robertson, and S. G. Mason, "The Hydrodynamic Behaviour of Paper-Making Fibres," *Pulp Paper Mag. Canada*, **59**, No. 5, 117 (1958).
Gardner, R. P., R. M. Felder, and T. S. Dunn, "Tracer Concentration Responses and Moments for Measurements of Laminar Flow in Circular Tubes," *Intern. J. Appl. Rad. Isotopes*, **24**, 235 (1973).
Han, T. S., "The Status of the Sheet Forming Process—A Critical Review," *Inst. Paper Chemi.*, Appleton, Wisc. (1965).
Harrison, R. E., R. M. Felder, and R. W. Rousseau, "Accuracy of Parameter Estimation by Frequency Response Analysis," *Ind. Eng. Chem. Process Design Develop.*, **13**, 389 (1974).
Labrecque, R. P., "The Effects of Fiber Cross Sectional Shape on the Resistance to the Flow of Fluids Through Fiber Mats," *TAPPI*, **51** (1968).
Letan, R., "On Vertical Dispersed Two-Phase Flow," *Chem. Eng. Sci.*, **29**, 621 (1974).
Levenspiel, O., and J. C. R. Turner, "The Interpretation of Residence-Time Experiments," *ibid.*, **25**, 1605 (1970).
Levenspiel, O., B. W. Lai, and C. Y. Chatlynne, "Tracer Curves and the Residence Time Distribution," *ibid.*, 1611 (1970).
Ljunggren, K., "Review of the Application of Radioactive Tracers in the Pulp and Paper Industry," in *Radioisotopes in the Pulp and Paper Industry* (Proceedings Panel Helsinki, 1967), pp. 39-51, I.A.E.A., Vienna (1968).
Mason, S. G., and R. St. J. Manley, "Fiber Motions and Flocculation," *TAPPI*, **37**, 494 (1952).
Metzner, A. B., "Non-Newtonian Technology: Fluid Mechanics, Mixing and Heat Transfer," *Advan. Chem. Eng.*, **1**, 77 (1956).
Mih, W., and J. Parker, "Velocity Profile Measurements and a Phenomenological Description of Turbulent Fiber Suspension Pipe Flow," *TAPPI*, **50**, 237 (1967).
Moller, K., G. G. Duffy, and A. L. Titchener, "The Laminar Plug Flow Regime of Paper Pulp Suspensions in Pipes," in *Svensk Papperstidning*, **74**, 829 (1971).
Moller, K., and G. G. Duffy, "Plug Flow of Pulp Suspensions: Comment," *TAPPI*, **57**, 123 (1974).
Moreira, R. M., "Dynamic Modeling of Paper Pulp Slurry Flow Using Radiotracers," Ph.D. thesis, N.C. State Univ., Raleigh (1976).
Nelson, R. W., "Approximate Theories of Filtration and Retention," *TAPPI*, **47**, 752 (1964).
Novosad, Z., and J. Ulbrecht, "Conversion in Chemical Reactions for Isothermal Laminar Flow of Non-Newtonian Liquids in a Tubular Reactor of Circular Cross-Section," *Chem. Eng. Sci.*, **21**, 405 (1965).
Osborne, F. T., "Purely Convective Models for Tubular Reactors with Non-Newtonian Flow," *ibid.*, **30**, 159 (1975).
Robertson, A. A., and S. G. Mason, "Specific Surface of Cellulose Fibers by the Liquid Permeability Method," *Pulp Paper Mag. Canada*, **50**, No. 12, 103 (1949).
Robertson, A. A., "Flow of Dilute Fiber Suspensions," *TAPPI*, **48**, 98A (1965).
Sanders, H. T., Jr., and H. Meyer, "Consistency Distributions in Turbulent Tube Flow of Fiber Suspensions," *ibid.*, **54**, 722 (1971).
Sankey, C. A., S. G. Mason, G. A. Allen, and W. R. Keating, "Application of Radioactive Tracers to Measurements of Fibre Flow and Distribution," *Pulp Paper Mag. Canada*, **52**, No. 3, 136 (1951).
Schweitzer, G., "Studie zur Kennzeichung von Papierfaserstoffen durch ihre Spezifische Oberflache," *Das Papier*, **29**, 9 (1975).
Sheppard, C. W., M. P. Jones, and B. L. Couch, "Effect of Catheter Sampling on the Shape of Indicator-Dilution Curves," *Circulation Res.*, **7**, 895 (1959).
Stamm, A. J., "Density of Wood Substance, Adsorption by Wood, and Permeability of Wood," *J. Phys. Chem.*, **33**, 398 (1929).
Stenuf, T. J., and K. P. Anumolu, "Plug Flow of Pulp Suspensions," *TAPPI*, **55**, 1387 (1972).
Wein, O., and J. Ulbrecht, "Residence Time Distribution in Laminar Flow Systems. II—Non-Newtonian Tubular Flow," *Collection Czechoslov. Chem. Commun.*, **37**, 3240 (1972).
Wen, C. J., and L. T. Fan, *Models for Flow Systems and Chemical Reactors*, Marcel Dekker, New York (1975).
Wrist, P. E., "Flow Properties of Fibrous Suspensions," in *Surfaces and Coatings Related to Paper and Wood*, by R. H. Merchessault, and C. Skaar, eds., Syracuse University Press, Syracuse, N.Y. (1967).
Zuber, N., "On the Dispersed Two-Phase Flow in the Laminar Flow Regime," *Chem. Eng. Sci.*, **19**, 897 (1964).

*Manuscript received January 23, 1978; revision received August 25, and accepted September 6, 1978.*

---

# Dynamic Response of the Carbon Dioxide Electrode

**TERRENCE L. DONALDSON**
and
**HARVEY J. PALMER**
Department of Chemical Engineering
University of Rochester
Rochester, New York 14627

**Complex relationships among multiple chemical species during unsteady diffusion and reaction are shown to cause hysteresis, *p*H dependent response rates, and general nonfirst-order transient behavior in agreement with common experimental observations. Response improvement by enzymic catalysis of the carbon dioxide hydration reaction also is considered.**

## SCOPE

**Potentiometric electrodes have become common analytical devices. Although their equilibrium behavior is reasonably well understood, their transient behavior is poorly characterized, and they often exhibit nonideal phenomena. An example is the carbon dioxide electrode (Stow, Baer, and Randall, 1957), which is an adaptation of the common glass membrane *p*H electrode in which the *p*H of a thin layer of bicarbonate solution in equilibrium with ambient carbon dioxide is measured. It is used routinely in blood gas analysis, in vivo blood studies, and respiratory gas analysis.**

---

Correspondence concerning this paper should be addressed to Terrence L. Donaldson.

0001-1541-79-2166-0143-$01.15.

Several studies have indicated that under some conditions the electrode exhibits memory and hysteresis, requires a very long time to equilibrate, and shows an increased response rate in the presence of the enzyme carbonic anhydrase (Severinghaus and Bradley, 1958, 1971; Severinghaus, 1968; Lunn and Mapleson, 1963; Fatt, 1964; Thatte, 1975; Grant, 1977). These paradoxical effects impede the accurate and efficient use of the device as an analytical tool.

The objective of the present investigation is to identify and quantify the fundamental phenomena which are responsible for the anomalous response characteristics of the carbon dioxide electrode. Experiments are conducted to demonstrate clearly the relationship between $p$H and the transient response rate of the electrode, particularly with regard to nonfirst-order response characteristics and hysteresis. A theoretical model is then developed to predict the transient behavior of the electrode. Incorporated in the model are transient multicomponent diffusion, chemical reaction, and nonlinear reaction equilibria. Special cases are considered which illustrate the contributions of these factors to the transient response characteristics of the carbon dioxide electrode. The general results, however, are relevant to the interpretation of response curves for other specific-ion electrodes.

## CONCLUSIONS AND SIGNIFICANCE

Experimental results confirm the nonfirst-order behavior, hysteresis, and response improvement with carbonic anhydrase observed by other investigators. These effects become more pronounced as the $p$H is increased ($P_{CO_2}$ is decreased). By changing the bicarbonate ion concentration in the sorbing solution, it is shown experimentally that the response rate is $p$H dependent, rather than carbon dioxide dependent as implied by other investigators. The presence of carbonic anhydrase reduces these nonfirst-order effects somewhat but does not entirely eliminate them. Both immobilized and homogeneous solution preparations of enzyme are used. The immobilized preparation is quite stable and is simple to use on a practical basis.

The governing transient multicomponent reaction and diffusion equations are solved for several important cases. It is shown that for constant bicarbonate ion concentration, the rate of the uncatalyzed carbon dioxide hydration reaction is sufficiently rapid relative to diffusion rates to maintain local chemical equilibrium in the bicarbonate layer. Hence, another explanation must be found for the mechanism by which carbonic anhydrase improves the response rate. In addition, the response is a simple exponential function (except at very short time), and no hysteresis is predicted.

When the bicarbonate-carbonate equilibrium and water dissociation are included, nonlinear and hysteresis effects are obtained owing to the complex nonlinear equilibrium relationship between $[H^+]$ and $[CO_2]$. The predicted hysteresis is in good agreement with the experimental data. This analysis is believed to be the first proper explanation and quantitative description of the hysteresis observed by all previous investigators. This system is another example of the fact that gas absorption and desorption with chemical reaction are not identical rate processes.

The mechanism by which the response is improved in the presence of carbonic anhydrase is not completely understood. It is possible that chemical reaction rate enhancement in the double layer region at the surface of the glass electrode could provide an alternate pathway for transport of $H^+$ (Palmer and Donaldson, 1978).

A variety of potentiometric electrodes for the measurement of specific ions and other chemical species have been developed and commercialized. The operation of these devices often depends on diffusion of one or more species and prior, simultaneous, or subsequent chemical reaction to convert one species to another chemical form which is sensed by the indicating electrode. An example is the urea electrode, which requires the enzyme urease immobilized within the electrode assembly to produce ammonium ions which are then detected by a cation specific electrode (Guilbault and Montalvo, 1970). Specific ion and enzyme electrodes have been reviewed by Gough and Andrade (1973) and Rechnitz (1975).

The steady state equilibrium behavior of these electrodes is reasonably well understood and is usually approximately Nernstian (Durst, 1969). The transient response is often somewhat slow, owing to the diffusional resistances and the finite rates of the chemical reactions. In principle it should be possible to improve the transient response characteristics by accelerating the chemical reaction rate via the addition of a catalyst (such as an enzyme). This improvement is anticipated, of course, only if the electrode response dynamics are limited in part by the chemical reaction rate and not limited solely by the diffusional rate.

With these ideas in mind, we began an experimental and analytical study of the response dynamics of the carbon dioxide electrode. This device is an adaptation of the common $p$H electrode in which a thin layer of aqueous bicarbonate solution is immobilized over the glass sensing membrane of the $p$H electrode, which in turn is covered by a gas permeable membrane such as Teflon or silicone rubber (details are discussed below). The equilibrium $p$H of the bicarbonate layer is determined by the carbon dioxide partial pressure in the ambient phase.

The transient response process requires the diffusion and chemical interconversion of carbon dioxide to $H^+$, $HCO_3^-$, and $CO_3^=$. The first-order rate constant for the carbon dioxide hydration process is about 0.04 $s^{-1}$ at 25°C, which means that the reaction has a half time of about 20 s. Since the experimentally observed electrode response rates are similar in magnitude to the reaction half time, it seems probable that the response rate can be increased by the addition of the enzyme carbonic anhydrase, which catalyzes the reversible carbon dioxide hydration reaction.

The use of carbonic anhydrase for this purpose is not new; other investigators have reported results which appear to be contradictory. Severinghaus and Bradley (1958) initially found that the enzyme had no effect on the re-

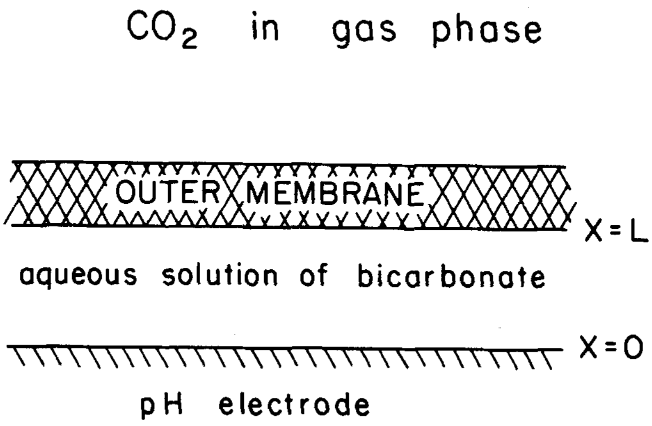

Fig. 1. Schematic diagram of CO$_2$ electrode.

sponse rate over the range 1.38 to 11.37% carbon dioxide in the gas phase but later said that the response may be accelerated by adding 1 mg/ml carbonic anhydrase (Severinghaus, 1968; Severinghaus and Bradley, 1971). On the other hand, Lunn and Mapleson (1963) suggested that, based on an electrical analogue model for the response, accelerating the reaction rate with a catalyst (for example, carbonic anhydrase) should affect the response rate only below 6% carbon dioxide. In addition, all these experimental studies, including Fatt (1964), report hysteresis; that is, the response curve for an increase in $P_{CO_2}$ is significantly different from the response curve for a decrease in $P_{CO_2}$. Our experimental results confirm all the observations made by other investigators. Sometimes the enzyme improved the transient response rate; sometimes it did not. Sometimes there was substantial hysteresis dependent on the direction of the $P_{CO_2}$ change; sometimes there was very little hysteresis. The hysteresis appeared as qualitative and quantitative differences in the shapes of the two response curves.

We have developed a theoretical model for the electrode response behavior based on transient diffusion and chemical reaction. The model successfully predicts the hysteresis in a quantitative manner. The experiments and analyses provide an interesting example of the complex interactions which can occur in transient diffusion and chemical reaction systems.

## THE CARBON DIOXIDE ELECTRODE

The essential components of a carbon dioxide electrode are shown schematically in Figure 1. A combination reference-*p*H electrode with a flat tip is covered by a nylon mesh matrix which contains an aqueous bicarbonate solution. The nylon mesh also contacts the reference junction of the combination electrode. An outer membrane, typically of silicone rubber or Teflon, holds the mesh and bicarbonate solution in place and prevents loss of the bicarbonate solution into the sample phase. The outer membrane is permeable to gases but impermeable to ions and liquids. Gases in the exterior sample phase will equilibrate with the bicarbonate solution in the electrode, and the dissolved carbon dioxide will react according to the net reactions

$$CO_2 + H_2O \underset{k_{-1}}{\overset{k_1}{\rightleftharpoons}} HCO_3^- + H^+ \qquad (1)$$

$$HCO_3^- \overset{\text{fast}}{\rightleftharpoons} H^+ + CO_3^= \qquad (2)$$

The equilibrium relationship between carbon dioxide and H$^+$ is determined by these two equations plus the dissociation of water. Since the bicarbonate layer is in contact with the *p*H electrode, the dissolved carbon dioxide concentration can be determined from the measured *p*H.

The transient response of the electrode following a step change in the partial pressure of carbon dioxide involves diffusion of carbon dioxide through the hydrophobic outer membrane, followed by diffusion and simultaneous chemical reaction in the stagnant bicarbonate layer. The *p*H electrode responds to the change in H$^+$ at the surface of the electrode.

The reaction in Equation (1) is catalyzed by carbonic anhydrase, whose properties may be found elsewhere (Maren, 1967; Donaldson and Quinn, 1974). Carbonic anhydrase is extremely efficient and increases the reaction rate by orders of magnitude when present in very small quantities. The enzyme may be incorporated into the bicarbonate layer either in homogeneous solution or chemically bound to the nylon mesh matrix.

## EXPERIMENTAL METHOD

Carbon dioxide electrodes were constructed from combination reference-*p*H electrodes having a flat tip (Markson #1207) and membrane replacement kits for commercial carbon dioxide electrodes (Instrumentation Laboratories #19030). The thickness of the outer silastic membrane and the nylon mesh support for the bicarbonate solution was determined to be approximately 0.01 cm each from micrometer measurements with the materials sandwiched between two glass cover slips.

The transient behavior of the electrode was dependent on the degree to which the silastic membrane was stretched and the nylon mesh matrix was compressed, influencing the overall permeability of the membrane-liquid sandwich to carbon dioxide. These factors limited the reproducibility among separate assemblies of the electrode to about ±20%. The reproducibility for consecutive experiments without diassembling the electrode was much better, about ±5%.

A mixture of carbon dioxide and nitrogen saturated with water vapor was directed onto the sensitive area of the carbon dioxide electrode. Flow rates of the saturated carbon dioxide and nitrogen were measured with rotameters before the gases were mixed. The electrode was connected to a *p*H meter with expanded scale capabilities, and the output was fed to a variable speed strip-chart recorder.

First the system was calibrated to determine the equilibrium relationship between $P_{CO_2}$ and *p*H. To observe the transient behavior, an equilibrium condition was established at a particular $P_{CO_2}$, and then the $P_{CO_2}$ was changed by increasing or decreasing the carbon dioxide flow rate manually with a needle valve. This process took about 1 s. The *p*H was recorded as a function of time until a new equilibrium was reached. The lag time in the gas flow system between the mixing point and impingement on the electrode was negligible. The 90% response of the *p*H electrode alone and the associated electronics and recorder was determined experimentally to be of the order of 2 s, which is consistent with other reported values (Markovic and Osburn, 1973). No specific correction or adjustment for this effect was made.

The $P_{CO_2}$ ranged from $5 \times 10^2$ to $2.5 \times 10^4$ N/m$^2$. The bicarbonate solution was 0.01 M KHCO$_3$ and 0.1 M KCl, as recommended by Severinghaus (1968) for suitable sensitivity and electrical stability. Some experiments were done with 0.1 M KHCO$_3$ and no potassium chloride. Bovine carbonic anhydrase was obtained from Sigma Chemical Co. (C-7500). Enzyme concentration in the bicarbonate solution ranged from 0.015 to 5.0 kg/m$^3$. The enzyme also was immobilized on the nylon mesh matrix by a glutaraldehyde cross linking technique (Broun et al, 1970; Donaldson, 1974), which involves soaking the mesh in a *p*H 7, 0.02 M phosphate buffer solution containing 1 kg/m$^3$ enzyme, 4 kg/m$^3$ bovine serum albumin, and 0.4 wt% glutaraldehyde, and then allowing the mesh to dry overnight at 278°K. The mesh was then soaked and rinsed well to remove loosely bound enzyme. Wawro and Rechnitz

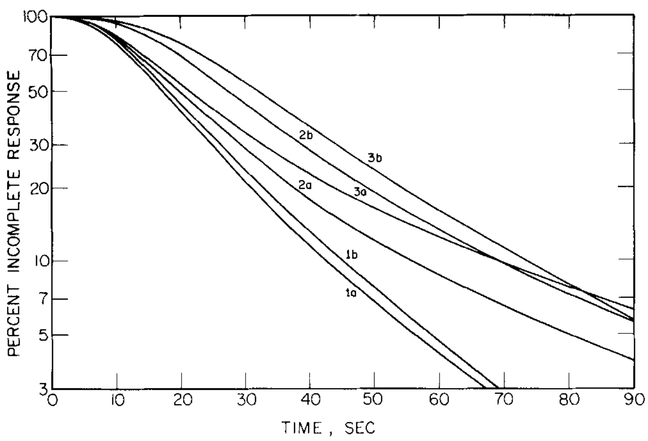

**Fig. 2. Experimental response curves which illustrate hysteresis and *p*H dependence. Bicarbonate concentration is 0.01 *M*. Initial and final *p*H values are 1*a*, 6.46 → 7.30; 1*b*, 7.30 → 6.46; 2*a*, 7.19 → 8.11; 2*b*, 8.10 → 7.18; 3*a*, 7.48 → 8.32; 3*b*, 8.32 → 7.45.**

(1976) have reported a pretreatment procedure for the nylon mesh which probably would increase the retention of enzyme. However, sufficient carbonic anhydrase was immobilized for our purposes without such special pretreatment.

## EXPERIMENTAL RESULTS

The transient response behavior is expressed as the logarithm of percentage incomplete response as a function of time. The percentage incomplete response (PIR) is defined in terms of $H^+$ concentration (not *p*H) and is given by

$$\text{PIR} = \frac{C_{\text{H}} - C_{\text{H}_1}}{C_{\text{H}_0} - C_{\text{H}_1}} \times 100$$

The function log (PIR) is linear with respect to time for simple transient diffusion of a nonreactive permeant in a finite layer (except at very short times) and provides a convenient basis for plotting our data.

Typical experimental response curves are shown in Figure 2 for an electrode containing 0.01 M $KHCO_3$ and 0.1 M KCl, with no enzyme. Curves 1, 2, and 3 represent different $P_{CO_2}$ ranges and consequently different initial and final *p*H values. The size of the step change in each case is about a factor of 6 in $P_{CO_2}$, as can be seen from the 0.8 unit differences in *p*H. In each case, curve *a* represents a *p*H increase ($P_{CO_2}$ decrease) and curve *b* a *p*H decrease ($P_{CO_2}$ increase) for the same two endpoints.

The response curves are qualitatively and quantitatively different for different *p*H regions and direction of the step change. The response rate decreases and the hysteresis increases as the *p*H increases. All the curves exhibit a tailing effect at long times which becomes more substantial as the *p*H increases.

The data in Figure 2 were obtained with one electrode assembly. As mentioned earlier, the quantitative results differ somewhat from one experimental assembly to another; however, the qualitative aspects described above were always present.

To determine if the varying response rates and hysteresis are functions of *p*H rather than of $P_{CO_2}$, the bicarbonate concentration in the electrode was changed while maintaining the same range of $P_{CO_2}$ values. Response curves are shown in Figure 3 for an electrode containing 0.1 M $KHCO_3$, no potassium chloride and no enzyme. The bicarbonate concentration is tenfold greater, and consequently the *p*H values are about one unit higher. Again, curves 1, 2, and 3 represent different *p*H end points, and curves a and b in each case represent a *p*H increase and a *p*H decrease, respectively. The qualitative features are identical with the curves in Figure 2, and the quantitative differences are more pronounced because of the higher *p*H values. These results indicate that it is in fact the *p*H, and not the $P_{CO_2}$, which is controlling the response rate and hysteresis.

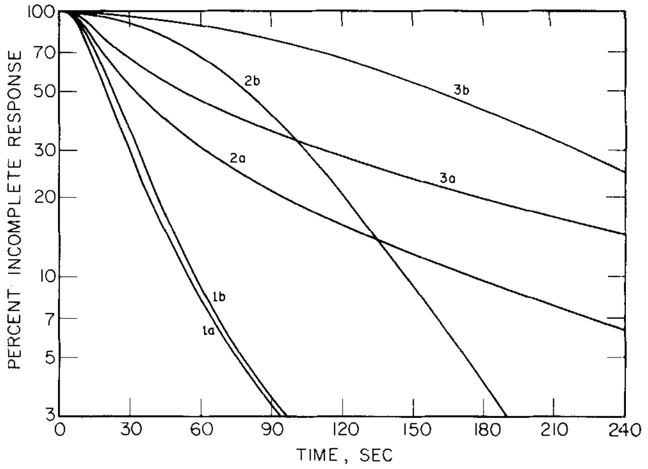

**Fig. 3. Experimental response curves at 10-fold higher bicarbonate concentration (0.1 M). Compare with Figure 2: hysteresis and *p*H dependence are more pronounced, although $P_{CO_2}$ values are approximately the same. Initial and final *p*H values are 1*a*, 7.43 → 8.20; 1*b*, 8.20 → 7.42; 2*a*, 8.28 → 9.10; 2*b*, 9.10 → 8.31; 3*a*, 8.50 → 9.28; 3*b*, 9.28 → 8.44.**

### Enzyme Electrode

In general, the response curves for electrodes containing 0.01 M $KHCO_3$, 0.1 M KCl, and 1 kg/m$^3$ carbonic anhydrase showed less hysteresis and somewhat steeper slopes at higher *p*H compared to the typical results without enzymes shown in Figures 2 and 3. The improvement in the presence of enzyme is difficult to quantify accurately because of the variability in electrode response associated with the mechanical assembly features mentioned earlier.

Experiments also were done with a round bulb shaped *p*H electrode for which the response improvement with enzyme was somewhat more significant (Thatte, 1975; Grant, 1977) but also difficult to quantify. The response curves with enzyme immobilized onto the nylon mesh support were identical to the curves with enzyme in homogeneous solution within experimental uncertainty. Results also were insensitive to the quantity of enzyme present. Nylon mesh preparations containing immobilized enzyme were stored in bicarbonate solution at 278°K and at ambient temperature in separate experiments and placed in electrode assemblies daily for response tests. In both cases, there was no deterioration of the electrode response for 25 days. The limiting factor was the physical integrity of the nylon mesh, which became weakened and torn after about 25 days of repeated handling. These results indicate that the loss of enzymatic activity is not likely to be a problem in practical applications. It is a well-known observation that many enzymes are more stable in immobilized forms than in homogeneous solutions (Wingard, 1972).

## MATHEMATICAL MODEL

A schematic diagram of the carbon dioxide electrode assembly is shown in Figure 1. The silastic membrane and bicarbonate layer are assumed to be uniformly thin and infinite in lateral extent. (The aspect ratio for the actual carbon dioxide probe is 100:1.) For simplicity, the total resistance to diffusion of carbon dioxide through the membrane and gas phase boundary layer is characterized by a constant mass transfer coefficient $k_m$ which incorporates the distribution coefficient for carbon dioxide between the membrane and the bicarbonate solution.

Initially, the system is at equilibrium characterized by the partial pressure of carbon dioxide in the gas phase $P_0$. At time equals zero, the partial pressure of carbon dioxide is instantaneously changed to $P_1$, and unsteady diffusion of carbon dioxide occurs in the system. For a step increase in $P_{CO_2}$, hydrogen ions are produced in the hydration reaction of carbon dioxide with water and in the dissociation of $HCO_3^-$ as the carbon dioxide diffuses into the bicarbonate solution. These hydrogen ions migrate to and adsorb onto the glass surface of the *p*H electrode (at $x = 0$) and thus alter its surface potential, which is monitored continuously by the associated electronic circuitry of the *p*H meter.

Unsteady diffusion and reaction of carbon dioxide, $HCO_3^-$, $CO_3^=$, $H^+$, and $OH^-$ must be considered to predict the transient response characteristics of the carbon dioxide electrode. The appropriate mass conservation equations for these species are

$$\frac{\partial C_C}{\partial t} = \mathcal{D}_C \frac{\partial^2 C_C}{\partial x^2} - k_1 C_C + k_{-1} C_B C_H \tag{3}$$

$$\frac{\partial C_B}{\partial t} = \mathcal{D}_B \frac{\partial^2 C_B}{\partial x^2} + k_1 C_C - k_{-1} C_B C_H - r_{CO3} \tag{4}$$

$$\frac{\partial C_{CO3}}{\partial t} = \mathcal{D}_{CO3} \frac{\partial^2 C_{CO3}}{\partial x^2} + r_{CO3} \tag{5}$$

$$\frac{\partial C_H}{\partial t} = \mathcal{D}_H \frac{\partial^2 C_H}{\partial x^2} + k_1 C_C - k_{-1} C_B C_H + r_{CO3} - r_W \tag{6}$$

$$\frac{\partial C_{OH}}{\partial t} = \mathcal{D}_{OH} \frac{\partial^2 C_{OH}}{\partial x^2} - r_W \tag{7}$$

These equations must be solved subject to the restrictions that the fluxes of carbon dioxide, $HCO_3^-$, $CO_3^=$, and $OH^-$ be zero at the surface of the glass sensing membrane ($x = 0$), and that the flux of $HCO_3^-$, $CO_3^=$, $H^+$, and $OH^-$ be zero at the silastic membrane: bicarbonate solution interface ($x = L$). Strictly speaking, the flux of $H^+$ is not zero at $x = 0$ because hydrogen ions must transfer to or from the glass surface of the *p*H electrode to alter its surface potential. However, because so few $H^+$ ions need to adsorb on the electrode surface to significantly alter the surface potential, the flux of $H^+$ at $x = 0$ will be considered equal to zero. The flux of carbon dioxide at $x = L$ is

$$\mathcal{D}_C \frac{\partial C_C}{\partial x} = k_m (C_{C_1} - C_C) \tag{8}$$

where $C_{C_1}$ is the concentration of carbon dioxide in equilibrium with the carbon dioxide partial pressure $P_1$.

Equations (3) through (8) are nonlinear and tightly coupled. Rather than attempt to solve this general set of equations numerically, we consider two special cases:

1. The effect of the carbon dioxide hydration reaction rate on electrode response is explored by considering a simplified model with negligible carbonate ion, constant bicarbonate ion concentration, and negligible buffering capacity of water. Results of this analysis reveal that the uncatalyzed hydration reaction is already sufficiently fast to establish local chemical equilibrium and a response rate controlled by diffusion.
2. The effects of bicarbonate ion dissociation and water dissociation are investigated for the special case of fast hydration reaction rate. The dissociation of bicarbonate to carbonate and the dissociation of water produce a nonlinear reaction equilibrium relationship between changes in dissolved carbon dioxide and $H^+$ concentrations. The analysis reveals that this nonlinear equilibrium relationship can cause apparent time delays, tailing, and hysteresis in the electrode response curve and that these nonfirst-order characteristics become increasingly more noticeable as the *p*H of the bicarbonate solution layer increases.

It is important to recognize that the nonlinear reaction equilibrium relationship applies to the incremental changes in the species concentrations accompanying an incremental change in dissolved carbon dioxide. This relationship determines the total quantity of carbon dioxide which must be transported in or out by diffusion to establish a new thermodynamic equilibrium state. These final equilibrium states may, in fact, exhibit an effectively linear relationship between dissolved carbon dioxide and $H^+$ when other species concentrations are sufficiently large or negligibly small.

### Effect of Carbon Dioxide Hydration Reaction Rate

To determine the effect of carbon dioxide hydration reaction rate on electrode response, we consider a model with negligible carbonate, constant bicarbonate concentration, and negligible buffering capacity of water. For these conditions, Equations (3) and (6) (with $r_{CO3} = r_W = 0$), together with the appropriate boundary conditions, describe the system's response. The equations in dimensionless form are

$$\frac{\partial C_C^*}{\partial \tau} = \frac{\partial^2 C_C^*}{\partial \xi^2} - N_K N_{EQ}(C_C^* - C_H^*) \tag{9}$$

$$\frac{\partial C_H^*}{\partial \tau} = N_D \frac{\partial^2 C_H^*}{\partial \xi^2} + N_K(C_C^* - C_H^*) \tag{10}$$

$$C_C^* = 1, \quad C_H^* = 1 \quad \text{at} \quad \tau = 0 \tag{11, 12}$$

$$\frac{\partial C_C^*}{\partial \xi} = 0, \quad \frac{\partial C_H^*}{\partial \xi} = 0 \quad \text{at} \quad \xi = 0 \tag{13, 14}$$

$$\frac{\partial C_H^*}{\partial \xi} = 0 \quad \text{at} \quad \xi = 1 \tag{15}$$

$$\frac{\partial C_C^*}{\partial \xi} + N_{BI} C_C^* = 0 \quad \text{at} \quad \xi = 1 \tag{16}$$

where (9) and (10) are the field equations for mass conservation of carbon dioxide and $H^+$, (11) and (12) are the initial conditions, (13) and (14) require zero flux of carbon dioxide and $H^+$ at the glass surface of the *p*H electrode, (15) is the zero flux condition for $H^+$ at the silastic membrane, and (16) equates the flux of carbon dioxide through the membrane to the flux into the bicarbonate solution.

An analytic solution to Equations (9) through (16) cannot be obtained. Therefore, an approximate solution was generated by the Galerkin method (see Finlayson, 1972) with expansion functions for $C_C^*$ and $C_H^*$ chosen to satisfy the associated uncoupled set of differential equations, in which the $C_H^*$ dependence is eliminated from (9) and the $C_C^*$ dependence is ignored in (10). Thus

$$C_C^* \approx \sum_{j=1}^{n} A_j(\tau) \cos \gamma_j \xi$$

$$C_H^* \approx B_0(\tau) + \sum_{j=1}^{n} B_j(\tau) \cos(j\pi\xi)$$

with

$$\gamma_j = N_{BI} \cot \gamma_j$$

$$A_j = \left[\frac{2}{\gamma_j}\sin\gamma_j\right] \Big/ [1 + N_{BI}/(\gamma_j^2 + N_{BI}^2)] \quad \text{at} \quad \tau = 0$$

$$B_0 = 1, \quad B_j = 0 \quad \text{for all } j > 0 \quad \text{at} \quad \tau = 0$$

In general, four-term expansions for $C_C^*$ and $C_H^*$ were needed to represent adequately the solution to Equations (9) to (16), except at very short times ($\tau < 0.05$) for which as many as twenty terms were necessary. Values of $\mathcal{D}_C = 2 \times 10^{-5}$ cm²/s, $\mathcal{D}_H = 9.5 \times 10^{-5}$ cm²/s, $k_1/k_{-1} = 6 \times 10^{-7}$M, and $C_B = 0.01$ M were used to compute values of $N_D = 4.75$ and $N_{EQ} = 6 \times 10^{-5}$. The value for the Biot number $N_{BI} = 1$ was estimated assuming negligible gas phase resistance, silastic membrane and bicarbonate solution layers of equal thickness of 0.01 cm, carbon dioxide diffusivity in the membrane of $2 \times 10^{-6}$ cm²/s, and a partition coefficient for carbon dioxide between the membrane and the bicarbonate solution of 10.

The theoretical predictions are shown in Figure 4 and reveal that the response of the model electrode follows a simple exponential decay at long times with no hysteresis, regardless of the value of the Damköhler number $N_K$. These results differ considerably from the experimental observations (see Figures 2 and 3) which show nonlinear phenomena at long times and hysteresis. Furthermore, the model provides no explanation for the reduction in electrode response rate with increasing *p*H which is observed experimentally. Finally, the analysis indicates that a value of $N_K > 10$ is sufficient to guarantee local chemical reaction equilibrium within the bicarbonate solution and a response rate which is determined by the rate at which $H^+$ ions can diffuse to the surface of the *p*H electrode. For the uncatalyzed carbon dioxide hydration reaction $k_1 = 0.037$ s$^{-1}$ and $N_K = 3\,100$, and addition of enzyme will further increase $N_K$. Therefore, based on this theoretical model, we should expect no improvement in electrode response with the addition of enzyme. Yet our experimental results and those of other investigators indicate that some enhancement does occur.

Clearly this simplified analysis is inadequate to describe the experimental observations, but it does show that finite reaction rate is not the explanation for the hysteresis and nonfirst-order behavior.

### Fast Reaction Limit with Bicarbonate and Water Dissociation

Lunn and Mapleson (1963) have proposed that the tailing in the electrode response curves at long times is due to the dissociation of $HCO_3^-$ to $H^+$ and $CO_3^=$, which results in a nonlinear equilibrium relationship between absorbed carbon dioxide and $H^+$ in solution. However, they did not consider the hysteresis phenomenon. Since the degree of $HCO_3^-$ dissociation is *p*H dependent, this effect may account for the reduction in response rate and the increase in hysteresis which is observed as the *p*H level in the bicarbonate solution is increased.

The theoretical analysis for the first case indicates that the uncatalyzed carbon dioxide hydration reaction is already sufficiently fast to guarantee local chemical equilibrium in the bicarbonate solution during the transient absorption of carbon dioxide. Thus, an estimate of the quantitative effects of bicarbonate and water dissociation on electrode response can be obtained by solving Equations (3) through (7) with the assumption of instantaneous chemical reaction. (The rates of the $HCO_3^-$ and water dissociation reactions are much higher than that for carbon dioxide hydration and may also be assumed to be infinite.) If local chemical reaction equilibrium obtains throughout the bicarbonate layer

$$K_B = C_H C_B / C_C \simeq 6.0 \times 10^{-7}\text{M} \tag{17}$$

$$K_{CO3} = C_H C_{CO3} / C_B \simeq 8.8 \times 10^{-11}\text{M} \tag{18}$$

$$K_W = C_H C_{OH} \simeq 10^{-14}\text{M}^2 \tag{19}$$

and Equations (3) through (7) may be combined to yield two independent field equations describing unsteady diffusion in the bicarbonate layer:

$$\frac{\partial}{\partial t}[C_C + C_B + C_{CO3}] = \frac{\partial^2}{\partial x^2}[\mathcal{D}_C C_C + \mathcal{D}_B C_B + \mathcal{D}_{CO3} C_{CO3}] \tag{20}$$

$$\frac{\partial}{\partial t}[C_H - C_{OH} - C_B - 2C_{CO3}] = \frac{\partial^2}{\partial x^2}[\mathcal{D}_H C_H - \mathcal{D}_{OH} C_{OH} - \mathcal{D}_B C_B - 2\mathcal{D}_{CO3} C_{CO3}] \tag{21}$$

With instantaneous homogeneous reactions, carbon dioxide effectively is consumed and $H^+$ produced at the silastic membrane: bicarbonate solution interface. At $x = L$, we may write

$$\mathcal{D}_C \frac{\partial C_C}{\partial x} = k_m (C_{C1} - C_C) - s_B$$

$$\mathcal{D}_B \frac{\partial C_B}{\partial x} = s_B - s_{CO3}$$

$$\mathcal{D}_{CO3} \frac{\partial C_{CO3}}{\partial x} = s_{CO3}$$

$$\mathcal{D}_H \frac{\partial C_H}{\partial x} = s_B + s_{CO3} - s_W$$

$$\mathcal{D}_{OH} \frac{\partial C_{OH}}{\partial x} = -s_W$$

Appropriate linear combinations of the above equations produce the desired boundary conditions at $x = L$:

$$\frac{\partial}{\partial x}[\mathcal{D}_C C_C + \mathcal{D}_B C_B + \mathcal{D}_{CO3} C_{CO3}] = k_m (C_{C1} - C_C) \tag{22}$$

$$\frac{\partial}{\partial x}[\mathcal{D}_H C_H - \mathcal{D}_{OH} C_{OH} - \mathcal{D}_B C_B - 2\mathcal{D}_{CO3} C_{CO3}] = 0 \tag{23}$$

In addition, the zero flux boundary condition at $x = 0$ for all species becomes

$$\frac{\partial}{\partial x}[\mathcal{D}_C C_C + \mathcal{D}_B C_B + \mathcal{D}_{CO3} C_{CO3}] = 0 \tag{24}$$

$$\frac{\partial}{\partial x}[\mathcal{D}_H C_H - \mathcal{D}_{OH} C_{OH} - \mathcal{D}_B C_B - 2\mathcal{D}_{CO3} C_{CO3}] = 0 \tag{25}$$

The solution of Equations (17) through (25) is complicated by the nonlinear relationships between the local molar concentrations of the diffusing species as given by Equations (17) through (19). This complication may be alleviated by assuming that all the molecular diffusivities are equal. Equations (21), (23), and (25) may now be solved to yield

$$C_B + 2C_{CO3} + C_{OH} - C_H = \text{constant} \equiv \beta \tag{26}$$

This result is consistent with the equilibrium conditions which determine the relationship between concentrations at initial and final equilibrium states. In addition, the use of a single diffusivity eliminates the need to consider forced diffusion in the electropotential field generated by unequal ion mobilities.

The consequences of the assumption of equal diffusivities are not obvious but are believed to be of secondary importance. In particular, recall that in the first case with a constant bicarbonate ion concentration and negligible carbonate ion and water dissociation, the additional assumption of equal diffusivities is unnecessary. Yet, if equal diffusivities are assumed for carbon dioxide and $H^+$ (that is, $N_D = 1$), the solution differs from the more general result only by a slight shift in the time scale.

Equation (26) may now be combined with Equations (17) through (19) to derive the following two relationships:

$$C_H = -(1 - \Gamma_C/\beta)(K_B/2) + [(1 - \Gamma_C/\beta)^2(K_B/2)^2 - K_B K_{CO3}(1 - 2\Gamma_C/\beta)]^{1/2} \quad (27)$$

$$C_C = \frac{1}{2}(\Gamma_C - \beta) + \frac{1}{2}[(\Gamma_C - \beta)^2 - (4\beta^2 K_{CO3}/K_B)(1 - 2\Gamma_C/\beta)]^{1/2} \quad (28)$$

where $\Gamma_C(x, t)$ is the local molar concentration of total carbon in solution and is equal to $C_C + C_B + C_{CO3}$. In deriving Equations (27) and (28), some obvious order of magnitude simplifications were employed which are valid for our experiments, such as $\beta >> C_{OH} - C_H$, $K_W/K_B C_C << 1$ and $K_B/4K_C >> 1$.

With the aid of Equation (28) and the assumption of equal diffusivities, Equations (20), (22), and (24) may be rewritten in dimensionless form together with the initial condition on $\Gamma_C$:

$$\frac{\partial \Gamma_C^*}{\partial \tau} = \frac{\partial^2 \Gamma_C^*}{\partial \xi^2} \quad (29)$$

$$\Gamma_C^* = 1 \quad \text{at} \quad \tau = 0 \quad (30)$$

$$\partial \Gamma_C^*/\partial \xi = 0 \quad \text{at} \quad \xi = 0 \quad (31)$$

$$\partial \Gamma_C^*/\partial \xi + \Gamma_C^* \{\overline{N}_{BI} + N_{BI}[\alpha(\tau) - \alpha(0)]\} = 0 \quad \text{at} \quad \xi = 1 \quad (32)$$

where

$$\alpha(\tau) = \frac{1}{2}(\Gamma_{C_1} + \Gamma_C - 2\beta + 8\beta K_{CO3}/K_B)/ \{[(\Gamma_{C_1} - \beta)^2 - (4\beta^2 K_{CO3}/K_B)(1 - 2\Gamma_{C_1}/\beta)]^{1/2} + [(\Gamma_C - \beta)^2 - (4\beta^2 K_{CO3}/K_B)(1 - 2\Gamma_C/\beta)]^{1/2}\}$$

and

$$\overline{N}_{BI} = \frac{1}{2} N_{BI}[1 + \alpha(0)]$$

Notice that Equation (32) is equivalent to the standard matching flux boundary condition (16) with a time dependent Biot number. The physical origin of this time dependent Biot number is the $p$H dependent (and hence time dependent) effective solubility of carbon dioxide expressed as total carbon in the aqueous solution. As carbon dioxide diffuses out of the aqueous layer, for example, the $p$H increases, and the effective carbon dioxide solubility increases. Hence, more and more carbon dioxide must leave the solution in order to establish the new equilibrium state. The anticipated result is a decrease in the response rate as the $p$H increases and vice versa for a $p$H decrease and carbon dioxide increase. Hysteresis and non-first-order behavior can also be expected owing to the nonlinear relationship between $\Gamma_C$ and $C_H$ seen in Equation (27). Consequently, even if Equation (32) had a constant effective Biot number and $\Gamma_C^*$ exhibited a simple exponential decay at long times, a plot of PIR vs. $\tau$ would tail because of the nonlinear relationship between $\Gamma_C$ and $C_H$.

To verify these expectations quantitatively, Equations (29) through (32) are solved approximately by the Galerkin method. Specifically

$$\Gamma_C^* \approx \sum_{j=1}^{n} A_j(\tau) \cos \gamma_j \xi$$

with

$$\gamma_j = \overline{N}_{BI} \cot \gamma_j$$

and

$$A_j(0) = \left[\frac{2}{\gamma_j} \sin \gamma_j\right] \Big/ [1 + \overline{N}_{BI}/(\gamma_j^2 + \overline{N}_{BI}^2)]$$

A boundary residual is then defined to approximate Equation (32); this residual is combined with the residual from the differential Equation (29), and the sum is multiplied by a weighting function and integrated in the usual manner to produce $n$ ordinary differential equations which determine the time dependence of $A_j$:

$$\frac{d}{dt} A_j = -\gamma_j^2 \delta_j A_j - 2\epsilon_j \sum_{\substack{m=1 \\ m \neq j}}^{n} A_m \cos \gamma_m \quad (33)$$

where

$$\delta_j = 1 + 2N_{BI}[\alpha(\tau) - \alpha(0)]/[\gamma_j^2 + \overline{N}_{BI}^2 + \overline{N}_{BI}]$$

and

$$\epsilon_j = \frac{N_{BI} \cos\gamma_j [\alpha(\tau) - \alpha(0)]}{1 + \overline{N}_{BI}/(\gamma_j^2 + \overline{N}_{BI}^2)}$$

The set of Equations (33) are then integrated numerically by the Runge-Kutta-Gill method. In general, a four-term expansion for $\Gamma_C^*$ was found to be adequate.

The results of these numerical computations are presented in Figures 5, 6, and 7. Figure 5 illustrates the influence of $p$H level on electrode response for a step change in carbon dioxide concentration equivalent to $\Delta p$H $= 0.5$. Response curves are identified by the initial and the final equilibrium $p$H. Notice that as the $p$H level is increased, the electrode response rate is reduced, and the response curves exhibit pronounced tailing and hysteresis similar to the experimental results.

The size of the step change, as well as the average $p$H in the bicarbonate solution, influences the degree of hysteresis, as shown in Figure 6. Calculations were done for step changes in carbon dioxide equivalent to changes in $p$H of 8.45 ↔ 8.55, 8.25 ↔ 8.75, and 8.0 ↔ 9.0 to maintain an average $p$H of 8.5 for all response curves. As expected, curvature and hysteresis are reduced as the size of the step change is decreased, and the response curves approach a straight line limit similar to the first case analysis for constant bicarbonate concentration (Figure 4).

The effect of nominal bicarbonate ion concentration is to determine the $p$H of the aqueous layer at a given carbon dioxide concentration. This is its only effect. Thus, the value of the bicarbonate concentration is irrelevant as long as results are presented in terms of $p$H. This feature can be proven algebraically; the ratios of carbon dioxide to $HCO_3^-$ and of $HCO_3^-$ to $CO_3^=$ are fixed once the $p$H is specified.

The response rate of the electrode is strongly influenced by the Biot number. The dimensionless time required to reach PIR $= 10\%$ for several values of $N_{BI}$ with $\Delta p$H $=$ 6.5 ↔ 7.0 is shown in Table 1. At this $p$H there is negligible hysteresis (Figure 5). However, while the absolute rate of response increases with increasing $N_{BI}$, the relative hysteresis and rate of response at different $p$H levels are altered only slightly by changes in the Biot number. Numerous combinations of $N_{BI}$ and an appropriate time scale

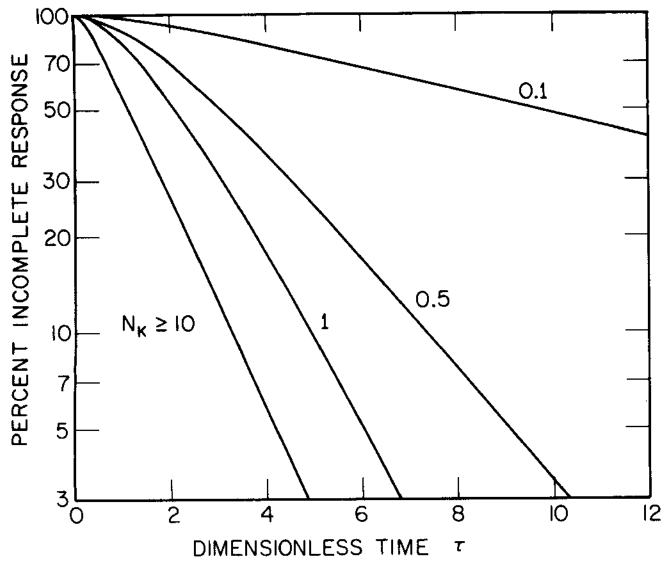

Fig. 4. Theoretical predictions for the effect of hydration reaction rate constant on the response rate. $N_D = 4.75$, $N_{EQ} = 6 \times 10^{-5}$, $N_{BI} = 1$.

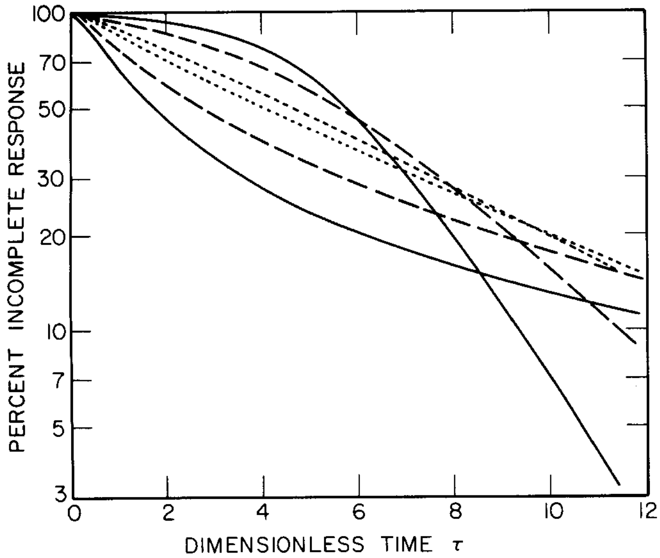

Fig. 6. Predicted dependence of response curves on magnitude of step change. Arithmetic average pH is 8.5 for all curves. Initial and final pH values are ——— 8.0 ↔ 9.0, - - - - 8.25 ↔ 8.75, . . . . 8.45 ↔ 8.55. $N_{BI} = 1$.

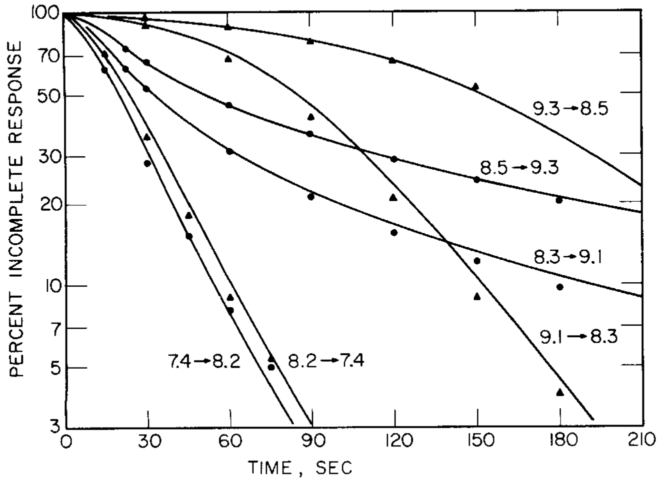

Fig. 7. Comparison of experimental and predicted response rates. Solid symbols represent points on experimental curves in Figure 3.

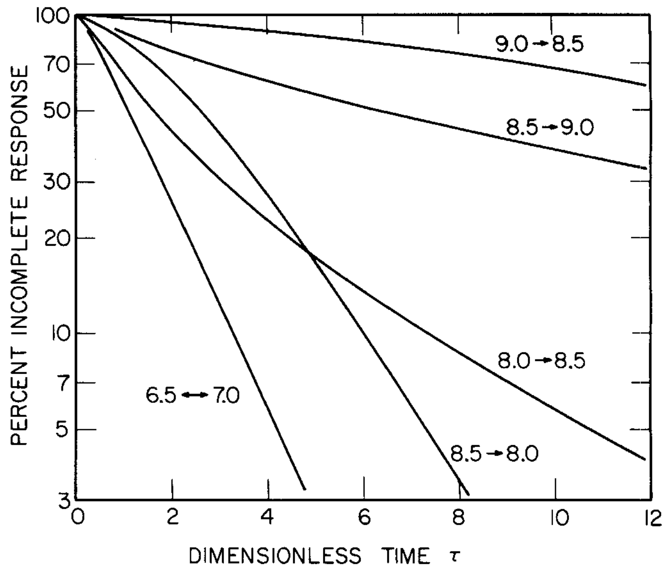

Fig. 5. Predicted response curves at reaction equilibrium for constant step size of 0.5 pH units. $N_{BI} = 1$.

TABLE 1. THE INFLUENCE OF $N_{BI}$ ON THE RATE OF RESPONSE OF THE CARBON DIOXIDE ELECTRODE $\Delta p$H = 6.5 ↔ 7.0

| $N_{BI}$ | τ for PIR = 10% |
|---|---|
| 0.1 | 24 |
| 0.2 | 12 |
| 0.4 | 6.7 |
| 1.0 | 3.3 |
| 10.0 | 1.0 |

$(L^2/\mathfrak{D})$ give essentially the same family of response curves for different $p$H levels when the results are presented in terms of real time.

The qualitative agreement between the model predictions and the experimental results is clear. We now want to determine to what extent this theoretical model can predict the experimental response curves quantitatively. Because the model assumes a constant diffusivity for all species, an appropriate diffusivity must be chosen. For the experiments with 0.1 M $KHCO_3$, the $p$H range is 7.4 to 9.3, and consequently the absorbed carbon dioxide is primarily converted to and diffuses as $HCO_3^-$. Therefore, a diffusivity of $1.2 \times 10^{-5}$ cm²/s was chosen, resulting in a value of $N_{BI} = 2.0$. With this value of $N_{BI}$ and $L = 0.01$ cm, the predictions compare favorably with the experiments. However, a somewhat better fit of the data may be obtained by choosing $N_{BI} = 10$ and appropriately increasing the time scale $(L^2/\mathfrak{D})$ by using $L = 0.025$ cm. Figure 7 presents the theoretical predictions (solid curves) for the experimental conditions in Figure 3. Experimental data points extracted from Figure 3 are also included to demonstrate the excellent quantitative agreement between the theoretical predictions and the experimental results over the full range of $p$H levels studied.

While our choices of $N_{BI}$ and a time scale are somewhat arbitrary, it is important to remember that smaller values of $N_{BI}$ with smaller values for $L$ give similar results, there is some uncertainty in our estimates of silastic membrane permeability to carbon dioxide and of the thickness of the bicarbonate layer, and absolute response rates were different from one electrode assembly to another, indicating that the actual bicarbonate layer thickness (and possibly the permeability of the membrane) varied.

Response data obtained by other investigators are also consistent with our model. For example, Severinghaus

(1968, Figure 9) shows response curves which are non-first-order and tail at long times. His curves are means of responses for carbon dioxide increase and decrease step changes, although he does not say how the means are calculated. The response rate increased as the bicarbonate concentration was decreased, corresponding to lower $p$H values, which is the behavior predicted by our model. Severinghaus also observed that "the 99% response requires only half as long for a fourfold increase as for a fourfold decrease of $P_{CO_2}$." This hysteresis effect may be seen in our Figures 3, 5, 6, and 7 in which the initially slower curve for a $p$H decrease ($P_{CO_2}$ increase) accelerates and crosses the curve for the change in the opposite direction and hence reaches high percent response values more quickly.

The reason for the improved response in the presence of carbonic anhydrase is not completely understood. The improvement is more noticeable at high $p$H than at low $p$H, which is consistent with the varied results reported by other investigators. It seems clear that the role of the enzyme is not catalysis of the hydration reaction in the bulk of the bicarbonate solution, since our analysis shows that the uncatalyzed reaction rate is already sufficiently rapid to have no influence on the response rate. It is possible that the enzyme effects are associated with transport in the electrostatic double layer at the glass electrode surface. We have shown (Palmer and Donaldson, 1978) that chemical reaction rates in this region can influence electrode response rates. Double-layer effects are probably small in our experimental systems because of the relatively high ionic strength, but the response improvement with enzyme is also small.

## ACKNOWLEDGMENT

This work was supported in part by a grant from the U.S. Public Health Service. We thank Dileep Thatte and David Grant for their contributions to the initial experimental study.

## NOTATION

$A_j$ = time dependent coefficients in the expansion solution for $C_C^*$
$B_j$ = time dependent coefficients in the expansion solution for $C_H^*$
$C$ = molar concentration in bicarbonate solution layer
$C^*$ = $(C - C_1)/(C_0 - C_1)$ = dimensionless concentration in bicarbonate solution layer
$\mathcal{D}$ = molecular diffusivity
$K$ = equilibrium constant
$k_m$ = mass transfer coefficient for outer membrane
$k_1$ = forward hydration reaction rate constant
$k_{-1}$ = reverse hydration reaction rate constant
$L$ = thickness of the bicarbonate solution layer
$N_{BI}$ = $k_m L/\mathcal{D}_C$ = dimensionless mass transfer coefficient for the outer membrane (Biot number)
$\overline{N}_{BI}$ = Biot number defined by Equation (32)
$N_D$ = $\mathcal{D}_H/\mathcal{D}_C$ = diffusivity ratio
$N_{EQ}$ = $k_1/C_B k_{-1}$ = dimensionless hydration equilibrium constant
$N_K$ = $k_{-1} C_B L^2/\mathcal{D}_C$ = dimensionless reaction rate constant (Damköhler number)
$P$ = partial pressure of carbon dioxide in ambient phase ($P_{CO_2}$)
$r$ = local molar rate of production per unit volume by chemical reaction
$s$ = local molar rate of production per unit area by chemical reaction
$t$ = time
$x$ = distance from glass surface of $p$H electrode

### Greek Letters

$\beta$ = constant defined by Equation (26)
$\Gamma_C$ = $C_C + C_B + C_{CO3}$ = local molar concentration of total carbon in solution
$\Gamma_C^*$ = $(\Gamma_C - \Gamma_{C_1})/(\Gamma_{C_0} - \Gamma_{C_1})$
$\xi$ = dimensionless $x$ coordinate = $x/L$
$\tau$ = dimensionless time = $t\mathcal{D}_C/L^2$

### Subscripts

B = bicarbonate ion
C = carbon dioxide
CO3 = carbonate ion
H = hydrogen ion
OH = hydroxyl ion
W = water
0 = initial equilibrium state
1 = final equilibrium state

### Superscripts

* = dimensionless variable

## LITERATURE CITED

Broun, G., E. Selegny, C. Tran-Minh, and D. Thomas, "Facilitated Transport of $CO_2$ Across a Membrane Bearing Carbonic Anhydrase," *FEBS Letters*, **7**, 223 (1970).

Donaldson, T. L., "Carbon Dioxide Transport and Carbonic Anhydrase Kinetics: Reaction and Diffusion Studies with Enzyme-Active Membranes," Ph.D. dissertation, Univ. Pa. (1974).

———, and J. A. Quinn, "Kinetic Constants Determined from Membrane Transport Measurements: Carbonic Anhydrase Activity at High Concentration," *Proc. Natl. Acad. Sci. USA*, **71**, 4995 (1974).

Durst, R. A., *Ion-Selective Electrodes*, National Bureau of Standards SP314, Washington, D.C. (1969).

Fatt, I., "Rapid-Responding Carbon Dioxide and Oxygen Electrodes," *J. Appl. Physiol.*, **19**, 550 (1964).

Finlayson, B. A., *The Method of Weighted Residuals and Variational Principles*, Academic Press, New York (1972).

Gough, D. A., and J. D. Andrade, "Enzyme Electrodes," *Science*, **180**, 380 (1973).

Grant, D. C., "Response Dynamics of the $P_{CO_2}$ Electrode," M.S. thesis, Univ. Rochester, N.Y. (1977).

Guilbault, G. G., and J. G. Montalvo, "An Enzyme Electrode for the Substrate Urea," *J. Am. Chem. Soc.*, **92**, 2533 (1970).

Lunn, J. N., and W. W. Mapleson, "The Severinghaus $P_{CO_2}$ Electrode: A Theoretical and Experimental Assessment," *Brit. J. Anaesth.*, **35**, 666 (1963).

Maren, T. H., "Carbonic Anhydrase: Chemistry, Physiology, and Inhibition," *Physiol. Rev.*, **47**, 595 (1967).

Markovic, P. L., and J. O. Osburn, "Dynamic Response of Some Ion-Selective Electrodes," *AIChE J.*, **19**, 504 (1973).

Palmer, H. J., and T. L. Donaldson, "Transient Diffusion and Reaction of Ions in an Electrostatic Double-Layer: Application to the Response of Potentiometric Electrodes," submitted to *Chem. Eng. Sci.*, for publication (1978).

Rechnitz, G. A., "Membrane Bioprobe Electrodes," *Chem. Eng. News*, **35** (Jan. 27, 1975).

Severinghaus, J. W., "Measurements of Blood Gases: $P_{O_2}$ and $P_{CO_2}$," *Ann. N.Y. Acad. Sci.*, **148**, 115 (1968).

———, and A. F. Bradley, "Electrodes for Blood $P_{O_2}$ and $P_{CO_2}$ Determination," *J. Appl. Physiol.*, **13**, 515 (1958).

———, *Blood Gas Electrodes or What the Instructions Didn't Say*, Radiometer, Copenhagen (1971).

Stow, R. W., R. F. Baer, and B. F. Randall, "Rapid Measurement of the Tension of Carbon Dioxide in Blood," *Arch. Phys. Med.*, **38**, 646 (1957).

Thatte, D., "Response Dynamics of the Enzymatic $P_{CO_2}$ Electrode," M.S. thesis, Univ. Rochester, N.Y. (1975).

Wawro, R., and G. A. Rechnitz, "Immobilized Enzyme Electrode for L-Asparagine," *J. Membrane Sci.*, **1**, 143 (1976).

Wingard, L. B., ed., *Enzyme Engineering*, Interscience, New York (1972).

*Manuscript received May 1, 1978; revision received September 14, and accepted October 5, 1978.*